Arabian Journal of Chemistry (2023) **16**, 105134

King Saud University

Arabian Journal of Chemistry

www.ksu.edu.sa
www.sciencedirect.com

ORIGINAL ARTICLE

One-pot preparation of environmentally friendly, high demulsification rate and novel functional magnetic demulsifier: Used for oil and water separation in crude oil emulsion

Xinlei Jia [a,b], Lixin Wei [b], Mingming Fu [a], Chao Liu [b], Yuxin Gu [b], Weining Qin [b], Lin Zhang [b], Xiaoheng Geng [a], Haiying Guo [a]

[a] *Department of Chemical Engineering and Safety, Binzhou University, Binzhou 256603, China*
[b] *School of Petroleum Engineering, Northeast Petroleum University, Daqing 163318, China*

Received 24 April 2023; accepted 2 July 2023
Available online 6 July 2023

KEYWORDS

Carbon nanospheres;
Fe_3O_4;
Fluorinated polyether;
Magnetic demulsifier;
Mechanism of demulsification

Abstract In this paper, a novel functional magnetic nano-demulsifier with efficient oil–water separation and recyclability was prepared by one-pot method. Magnetic fluorinated polyether composite demulsifier (Fe_3O_4@C-F) was prepared by combining Fe_3O_4 as magnetic matrix with carbon nanospheres and grafting fluorinated polyether. The morphology and structure of the composites were analyzed by scanning electron microscopy (SEM), Fourier transform infrared spectroscopy (FTIR) and transmission electron microscopy (TEM). The results showed that carbon nanospheres and fluorinated polyether were successfully compounded on Fe_3O_4, and the crystallinity of the composites was improved. The demulsification experiment and recovery performance test were carried out with the self-made crude oil emulsion. The main factors affecting the demulsification performance of demulsifier and its demulsification mechanism were discussed. The results showed that the demulsification effect of Fe_3O_4@C-F was the best when the dosage was 600 ppm, 65 °C, 120 min and pH value was 6. The demulsification rate could reach 96.68 %, and the oil–water interface was clear. Fe_3O_4@C-F had magnetic response, and could be recycled and reused 5 times from two-phase system under external magnetic field. The application of carbon materials in the field of

E-mail address: 18434362466@163.com (X. Jia)

Peer review under responsibility of King Saud University.

Production and hosting by Elsevier

https://doi.org/10.1016/j.arabjc.2023.105134

oil–water separation has injected a new power source for the application of carbon nanomaterials in the field of demulsifiers.

1. Introduction

In recent years, all kinds of petroleum products have become an integral part of modern human life. Especially since 2020, affected by the outbreak of COVID-19 pandemic, the global economy has deteriorated sharply, and the dependence of crude oil on foreign countries has been increasing in many countries (He et al., 2021; Shuying and Kun, 2021). A large number of emulsions will be produced during the exploitation and transportation of crude oil (Huang et al., 2019; Khan et al., 2019; Zhang et al., 2021). These stable emulsions reduce the service life of the equipment through corrosion, and the oily wastewater discharged can pollute the environment (Velayati and Nouri, 2021; Wang and Zhang, 2016). Therefore, the treatment of emulsions is facing a more severe test. However, conventional demulsifiers have problems such as large dosage of reagents, secondary pollution, and difficulty in recycling (Li et al., 2013; Hjartnes et al., 2019). Therefore, it is of great significance to develop new functional magnetic demulsifiers with small dosage of reagents, good demulsification effect, and recoverability.

The conventional unifurcated polyether demulsifier has posed challenges in fulfilling the requirements for oilfield utilization due to its drawbacks of substantial dosage and elevated demulsification temperature. Fluorinated surfactant is one of the most active surfactants found at present. It has high surface activity, high thermal stability, high chemical inertness, and hydrophobic and oil-repellent properties (Alves et al., 2020; Hu et al., 2017). In the realm of oil–water separation, the remarkable capability of fluorinated surfactants to substantially diminish the surface tension of both aqueous and organic solvent systems even at low concentrations has garnered considerable interest. Moreover, their applicability in diverse settings such as acidic, alkaline, highly oxidizing, and thermally demanding environments further accentuates their significance (Bélarbi et al., 2010; Zhang et al., 2016; Peyre, 2009). Our team has successfully introduced fluorine element into the molecular structure of demulsifier in the early stage (Zhang et al., 2022; Wei et al., 2021; Geng et al., 2022). The lipophilic segment is generated by the polymerization of bisphenol AF and propylene oxide, and then the hydrophilic ethylene oxide segment is polymerized on this basis to obtain the fluorinated linear block polyether surfactant, and the ideal demulsification effect is achieved. Under the context of PM200 crosslinking modification, the demulsification properties of linear and branched polyethers were examined by a team of researchers hailing from Shandong University (Yin, 2014). The results show that linear polyether micelles aggregate to form larger micelles by bridging the protonated water molecules with ether oxygen atoms in PEO, and the modified multi-branched polyether has good demulsification effect on offshore crude oil. The above findings demonstrate that the incorporation of functional groups into the side chain of polyethers enhances its functionality while preserving the exceptional properties of the main chain. This approach facilitates the development of polymer materials with catalytic activity, surface activity, and responsive properties, aligning with the inevitable trajectory for polyether materials to cater to market demands and advancements in novel technologies (Guo et al., 2021; Suhaimin et al., 2021).

Although the functional fluorinated polyether demulsifier has remarkable effect on emulsion separation, it is also difficult to recover and easy to cause secondary pollution. Nanomaterials have emerged in the application of demulsifiers due to their special surface properties, scale effect and macroscopic ion tunneling effect (Gasanov et al., 2019; Nab and Aaa, 2022; Nikkhah et al., 2015; Huang et al., 2019). Magnetic nanoparticles, as an emerging class of materials, encompass not only the intrinsic surface and size effects observed in conventional nanoparticles but also manifest distinct magnetic responsiveness. This magnetic responsiveness enables efficient recycling of magnetic nanoparticles through external magnetic fields. (Mu et al., 2022; Zhou et al., 2021). The modified functional magnetic demulsifier can effectively solve the problems of large dosage of traditional chemical demulsifier and difficult recovery after reaction. Compared with other applications, the application of magnetic nanoparticles in oil–water emulsion demulsification started late, but it has aroused many researchers' interest. Among various magnetic nanoparticles, Fe_3O_4 has magnetic responsiveness and hydrophilicity (Xie and Deng, 2017; Huan et al., 2019; Xu et al., 2021). Domestic and foreign scholars have used organic polymers and Fe_3O_4 to synthesize amphiphilic magnetic demulsifiers. They can be adsorbed on the oil–water interface membrane and replaced with natural emulsifiers on the interface membrane, reducing the stability of the interface membrane and achieving effective demulsification (Feng et al., 2021). In this study, Fang Shenwen et al. (Fang et al., 2017) employed propylene oxide-ethylene oxide block polyether (PPO-PEO) as a solvent, reducing agent, and surfactant for the one-step synthesis of a magnetic demulsifier known as PEMN. The synthesis involved reacting iron acetylpyruvate ($Fe(acac)_3$) with PPO-PEO, thereby achieving the desired magnetic demulsifying properties. Demulsification experiments showed that PEMN had excellent demulsification performance within 30 min when the demulsification temperature was 70°C and the demulsifier dosage was 0.625 g/L. In addition, PEMN can be recycled, showing excellent demulsification performance in three cycles, and the dehydration efficiency remains at 95%. Zhou Jingjing et al. (2021) synthesized a amphiphilic magnetic demulsifier (M−ANP) by grafting aliphatic alcohol non-ionic propylene oxide-ethylene oxide block polyether (ANP) onto the surface of epoxy-functionalized magnetite (Fe_3O_4) nanoparticles. Under the conditions of 2000 ppm addition and room temperature, the demulsification efficiency of M−ANP for W/O crude oil emulsion reached 95.5% in 2 min, and the demulsification rate of M−ANP could remain at 80% after one cycle in the cycle experiment, without further attenuation, which had good cycle recovery performance. The synergistic effect of ANP and MNPs provides us with inspiration on demulsification mechanism. For W/O emulsion, when the demulsifier molecule reaches the oil–water interface, the hydrophilic polyethylene oxide segment in the molecular structure of M−ANP at the oil–water interface will form hydrogen bonds with water, which will increase the adsorption capacity of M−ANP on the surface of water droplets, thus replacing the natural emulsifier molecule of the oil–water interface membrane and forming a more easily fractured oil–water interface membrane. Therefore, it is concluded that if the fluorinated polyether with better demulsification effect is used to replace ANP, a more perfect demulsification effect may be achieved. (Umar et al., 2020) covalently functionalized Fe_3O_4 nanoparticles with polyester bis (MPA) dendritic macromolecules, 2-hydroxy, and 1-azide dendritic macromolecules, and successfully synthesized amphiphilic polyester dendritic hydroxyl acid encapsulated Fe_3O_4 nanohybrid demulsifier (PEDHA-Fe_3O_4). The experimental findings demonstrate that when the demulsification temperature is set at 60 °C and the PEDHA-Fe_3O_4 dosage reaches 15 mg/L, the dehydration rate of PEDHA-Fe_3O_4 can reach a substantial 79.1%. Notably, even in the third demulsification cycle, the dehydration rate surpasses 50%. However, it is evident that the demulsification effect of PEDHA-Fe_3O_4 does not exhibit an optimal performance. We speculated that on the one hand, it might be because the demulsification effect of polyester dendritic hydroxyl acid was not high. On the other hand, PEDHA itself could not provide more sites

for the grafting of Fe_3O_4, resulting in only a small amount of PEDHA successfully wrapped on the surface of Fe_3O_4. Therefore, it is plausible to explore the incorporation of a material with a high specific surface area, as this would facilitate the provision of additional grafting sites for Fe_3O_4. Obviously, carbon nanospheres with low density, high strength, high specific surface area, thermal stability and chemical stability are suitable choices (Zhao et al., 2013; Zhao et al., 2019; He et al., 2016).

Given the scarcity of reports on carbon nanospheres and fluorinated polyether demulsifiers in oily wastewater treatment, our research team has taken a step further to develop novel environmentally friendly magnetic demulsifiers. This development builds upon our previous success in demonstrating the efficient demulsification rates achieved by fluorinated polyether demulsifiers for oil–water separation in crude oil emulsions. A novel magnetic demulsifier was synthesized by combining Fe_3O_4 with carbon nanospheres and grafting fluorinated polyether. The morphology and structure of this demulsifier were characterized, and the factors affecting demulsification and recovery performance were explored. The demulsification effect and demulsification mechanism of the demulsifier were studied by bottle test method, and the unexpected results were obtained. When the dosage was 600 ppm, 65 °C, 120 min and pH value was 6. The demulsification rate could reach 96.68%, and the oil–water interface was clear. Fe_3O_4@C-F had magnetic response, and could be recycled and reused 5 times from two-phase system under external magnetic field. It provides theoretical support for the efficient treatment of crude oil emulsion in China's petrochemical field and the environmental protection production of oilfields, and lays a foundation for the practical promotion of magnetic demulsifiers in oilfield demulsification.

2. Experimental

2.1. Materials

Fluorinated polyether was prepared according to the report. (Zhao et al., 2019) Fe(acac)3 was purchased from Shanghai Aladdin Industrial Co., Ltd., China. Oleic acid, oleylamine and carbon spheres were purchased from Shanghai McLean Biochemical Technology Co., Ltd. Benzyl Ether was purchased from Merck Chemical. All chemicals used in the production process are analytical grade. The dehydrated crude oil is supplied by a heavy oil block in Liaohe Oilfield. The physical and chemical properties are shown in Table 1.

2.2. One-pot preparation of magnetic demulsifier

The preparation process of carbon nanospheres, fluorinated polyether and Fe_3O_4-F can be found in the attachment.

Fe_3O_4@C-F was prepared by one-pot method (see Fig.1). Firstly, 0.001 mol ferric acetylacetonate, 0.003 mol oleic acid, 0.003 mol oleylamine, 0.1 g carbon nanospheres and 5 g fluorinated polyether were added into the beaker, and then the solvent dibenzyl ether was added. Subsequently, the contents in the beaker were subjected to thorough stirring and ultrasonic dispersion for a duration of 30 min. Following this, the reagents present in the beaker were transferred into the reactor, while simultaneously purging the reactor with nitrogen to eliminate any residual air. The reaction kettle was placed in a muffle furnace at 230 °C for 5 h. After the insulation experiment, remove the reactor, placed in the air naturally cooled. The product in the kettle was taken out, and the magnetic demulsifier product was separated by magnet, and the 1:1 vol mixture of ethanol and n-hexane was added to the product to clean the magnetic demulsifier product for 3–5 times. Finally, the product was dried at 60 °C for 12 h to obtain magnetic demulsifier.

2.3. Preparation of crude oil emulsion

Oil in water (O/W) emulsion with mass fraction of 1% was prepared. NaCl was dissolved in deionized water (5 mol/L, NaCl) to prepare brine, and then the mixture of crude oil (5 mL) and brine (495 mL) was heated to 60 °C, and constant temperature 20 min, 11,000 rpm stirring 20 min, stable O/W emulsion was obtained. The obtained water-in-oil emulsion can be stable at room temperature for at least 24 h.

2.4. Demulsification performance test

According to SY-T 5281–2000, the demulsification performance of fluorinated polyether, carbon nanospheres, Fe_3O_4, Fe_3O_4@C, Fe_3O_4-F and Fe_3O_4@C-F was evaluated by bottle test. First, the pre-configured crude oil emulsion is packed separately, each test tube is loaded with 20 mL emulsion, and then placed in a 65 °C water bath for 5 min to prevent droplet solidification in the emulsion. Then, according to the experimental requirements, the pre-configured demulsifier solution was added. It was heated in a 65 °C water bath for 5 min, and then the test tube was taken out. The test tube was shaken back and forth for 100 times within 1 min, so that the demulsifier and crude oil emulsion were completely mixed. Finally, the test tube was placed in a 65 °C water bath for static settlement, and the demulsification effect was observed after 5 min, 15 min, 30 min, 60 min, 90 min and 120 min, respectively.

2.5. Performance test of demulsification recovery

The recyclability of Fe_3O_4@C-F magnetic demulsifier was evaluated by reuse times. After the demulsification experiment, the obtained reagent was subjected to an external magnetic field to recover the Fe_3O_4@C-F magnetic demulsifier. The recovered product was washed with n-hexane, and then washed with an ultrasonic cleaner for 15 min. The demulsifier was fully dispersed, and then recovered through an external magnetic field, and washed three to four times until the solution was colorless and transparent. Finally, the product was dried in a vacuum drying oven at 60 °C for 6 h, and the next experiment was repeated.

Table 1 Basic physical properties of crude oil produced in a block of Liaohe Oilfield.

Density $kg{\cdot}m^{-3}$	Dynamic Viscosity (50 ℃) m Pa·s	Gum %	Asphaltene%	Acid value mg $KOH{\cdot}g^{-1}$	Pour point ℃	moisture content%
943.0	180.2	22.98	12.75	2.45	17	35.82

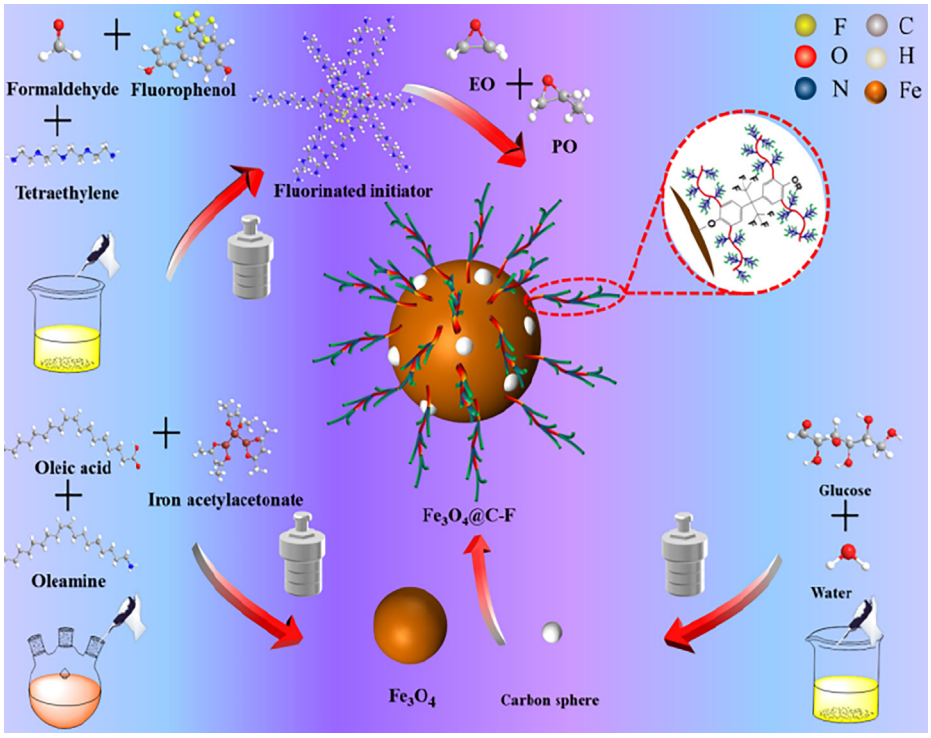

Fig. 1

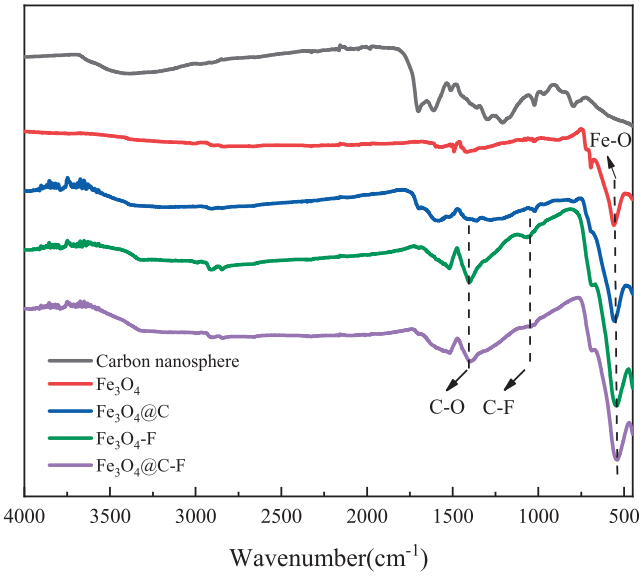

Fig. 2 FTIR of different materials.

3. Result and discussion

3.1. FTIR of different materials

Fig. 2 shows the infrared spectra of carbon nanospheres, Fe_3O_4 and their composites. The FTIR spectra of carbon nanospheres show that there are a large number of functional groups on the surface of carbon nanospheres. A wide absorption peak at 3421 cm^{-1} corresponds to the stretching vibration peak of —OH, a vibration absorption peak at 1700 cm^{-1} corresponds to the vibration peak of C═O, a vibration absorption peak at 1611 cm^{-1} corresponds to the vibration peak of C═C, a bending vibration peak at 1370 cm^{-1} corresponds to the vibration peak of C—O, and a stretching vibration peak at 1298 cm^{-1} and 1209 cm^{-1} corresponds to the vibration peak of C—OH. Comparing the carbon nanospheres with Fe_3O_4@C, it can be found that in addition to the functional groups of carbon nanospheres, Fe—O groups also appear at 560 cm^{-1}, corresponding to Fe^{3+} and Fe^{2+}, indicating that Fe_3O_4 and carbon nanospheres are successfully compounded. In addition, the intensity of the characteristic peaks of all functional groups except Fe—O groups of Fe_3O_4@C is obviously weakened because the carbon nanospheres are attached to Fe_3O_4, thus weakening its intensity. In the FTIR spectra of Fe_3O_4@C-F, —CH and $—CH_2$ stretching vibration absorption peaks appears at 2912 cm^{-1} and 2840 cm^{-1}, respectively, and C—F bond stretching vibration absorption peak appears at 1061 cm^{-1}, indicating that fluorinated polyether is successfully compounded on the surface of Fe_3O_4@C.

3.2. Morphology characterization of different materials

Fig. 3(a–c) is the SEM image of carbon nanospheres, Fe_3O_4, Fe_3O_4@C-F and the TEM image of Fe_3O_4@C-F. It can be seen from Fig. 3(a) that the shape of carbon nanospheres is spherical, the particle size is uniform, and the dispersion is good. The shape of Fe_3O_4 in Fig. 3(b) is also spherical and evenly dispersed. In Fig. 3(c), Fe_3O_4@C-F is spherical but the surface is not smooth. The surface of the sphere is obviously wrapped by a grayish white spherical shell, and the sphere has good dispersion. Fe_3O_4@C-F particles were further

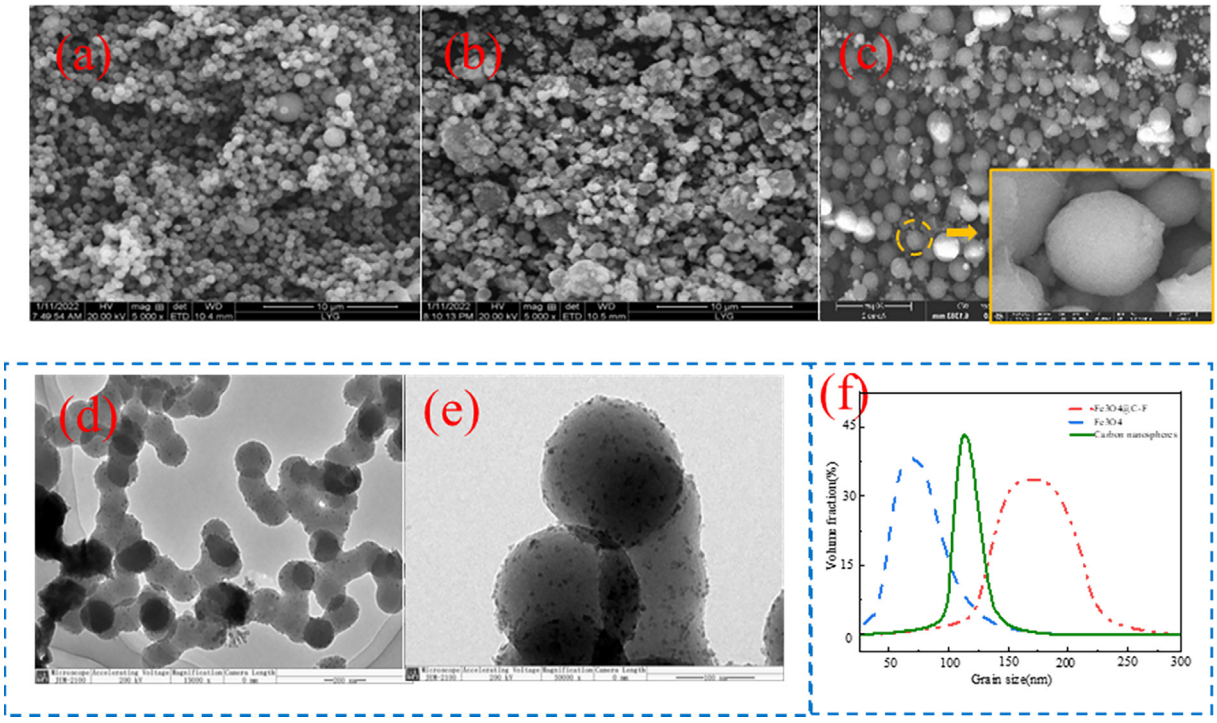

Fig. 3 SEM of carbon nanospheres, Fe_3O_4 and Fe_3O_4@C-F, TEM of Fe_3O_4@C-F, particle size of carbon nanospheres, Fe_3O_4 and Fe_3O_4@C-F. (a) SEM of carbon nanospheres, (b) SEM of Fe_3O_4, (c) SEM of Fe_3O_4@C-F, (d) (e) TEM of Fe_3O_4@C-F, (f) particle size of carbon nanospheres, Fe_3O_4 and Fe_3O_4@C-F.

observed by TEM and Fe_3O_4@C-F was determined by particle size analyzer. The visual representation in Fig. 3(d) and (e) clearly shows that carbon nanospheres are uniformly attached to the surface of Fe_3O_4 nanoparticles. Furthermore, fluorinated polyether molecules are tightly encapsulated within the outer layer of Fe_3O_4@C-F, resulting in a relatively uniform morphology. According to the particle size distribution (Fig. 3(f)), the average particle size of Fe_3O_4 is 63.2 nm, the average particle size of carbon spheres is 119.6 nm, and the average particle size of Fe_3O_4@C-F is 163.7 nm. The successful combination of carbon nanospheres, Fe_3O_4 and fluorinated polyether molecules can be preliminarily judged by analyzing the morphology of Fe_3O_4@C-F particles. The successful combination of carbon nanospheres, Fe_3O_4 and fluorinated polyether molecules can be preliminarily judged by analyzing the morphology of Fe_3O_4@C-F particles.

3.3. X-ray photoelectron spectroscopy (XPS) of different materials

The elemental valence and chemical composition of Fe_3O_4@C-F were further studied by XPS. In the full spectrum of Fe_3O_4@G-F (Fig. 4a), the signals of Fe, F, O and C elements appear at about 709.29, 684.58, 527.92 and 283.33 eV, respectively. In the high-resolution Fe2p spectrum of Fe_3O_4@C-F (Fig. 4b), two dominant peaks at 710.13 and 723.55 eV belong to $Fe2p_{3/2}$ and $Fe2p_{1/2}$ spin orbit peaks. At the same time, the peaks at 713.00 and 726.32 eV are consistent with the Fe^{3+} ions of the Fe—O bond. Two peaks at 710.2 and 723.6 eV are assigned to Fe^{2+} ions. It can be seen from the C1s spectrum in Fig. 4(c) that C1s can be divided into two strong peaks and one weak peak, which are C—C/C—H, C—OH and O═C—O, respectively. The two peaks in the O1s peak separation spectrum (Fig. 4d) are C═O and C—O, respectively. The spectroscopic and crystallographic results support that fluorinated polyether and Fe_3O_4 nanoparticles are supported by carbon nanospheres.

3.4. Effect of demulsifier dosage on demulsification performance

Fig. 5 shows that the different effects of Fe_3O_4@C-F magnetic demulsifier at different dosage on demulsification performance at the experimental temperature of 65 °C. Fig. 5(a) shows that when the dosage of Fe_3O_4@C-F magnetic demulsifier is 600 ppm, the demulsification effect is the best, and the demulsification rate reaches 96.68%. It can be seen from the Fig. 5 (b) test tube in the figure that the solution is clear and the wall of oil droplets is less. With the increase of dosage, the solution clarity decreases and the wall of oil droplets increases. This indicates that Fe_3O_4@C-F magnetic demulsifier is a very effective demulsifier for oily wastewater. When the demulsifier dosage is less than 600 ppm, the demulsification rate increases with the increase of demulsifier dosage. When the demulsifier dosage is greater than 600 ppm, it decreases with the increase of demulsifier dosage. This is due to the amphiphilicity of Fe_3O_4@C-F, which means when the dosage of demulsifier reaches a certain level, the adsorption amount of demulsifier molecules on the oil–water interface will reach saturation.The continuous increase of dosage will thicken the oil–water film, resulting in more stable oil–water interface film and reducing demulsification efficiency (Zhang et al., 2018). Therefore, the optimum concentration of Fe_3O_4@C-F magnetic demulsifier is 600 ppm.

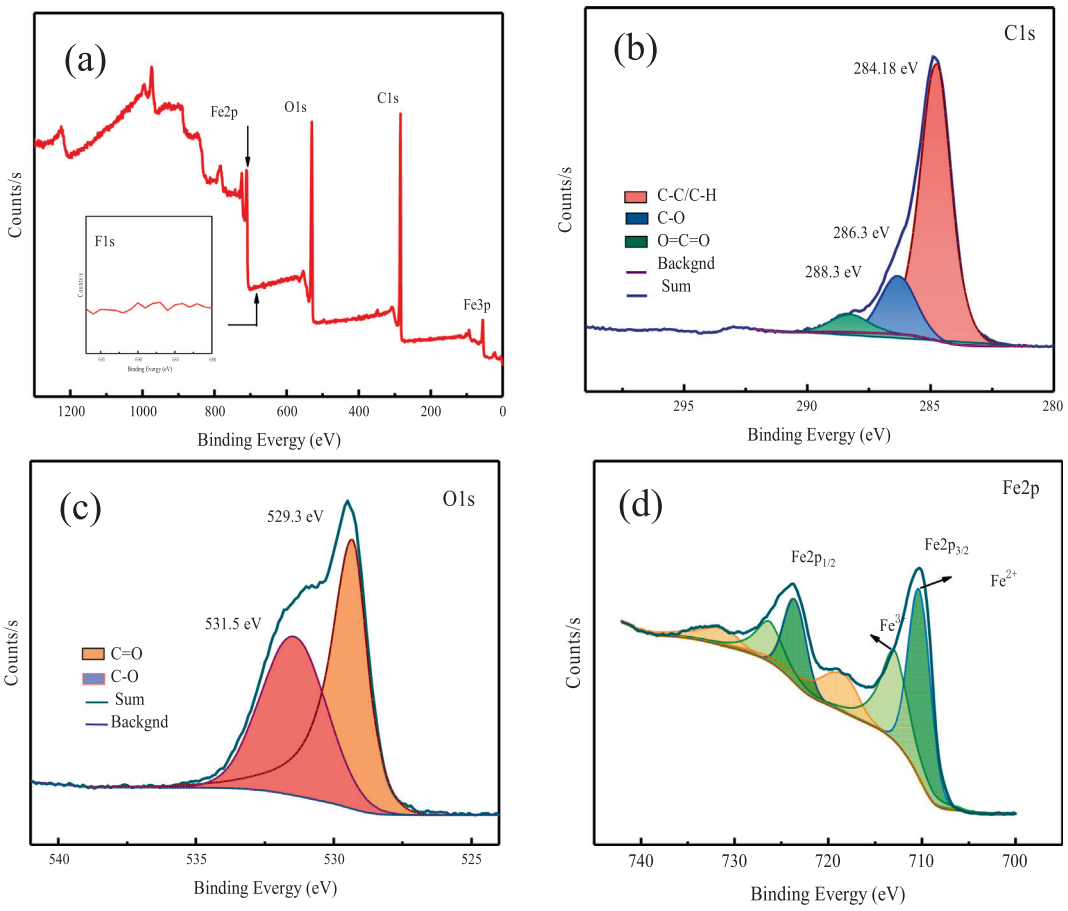

Fig. 4 (a) XPS of Fe_3O_4@C-F, (b) Peak diagram of Fe2p, (c) Peak diagram of O1s, (d) Peak diagram of C1s.

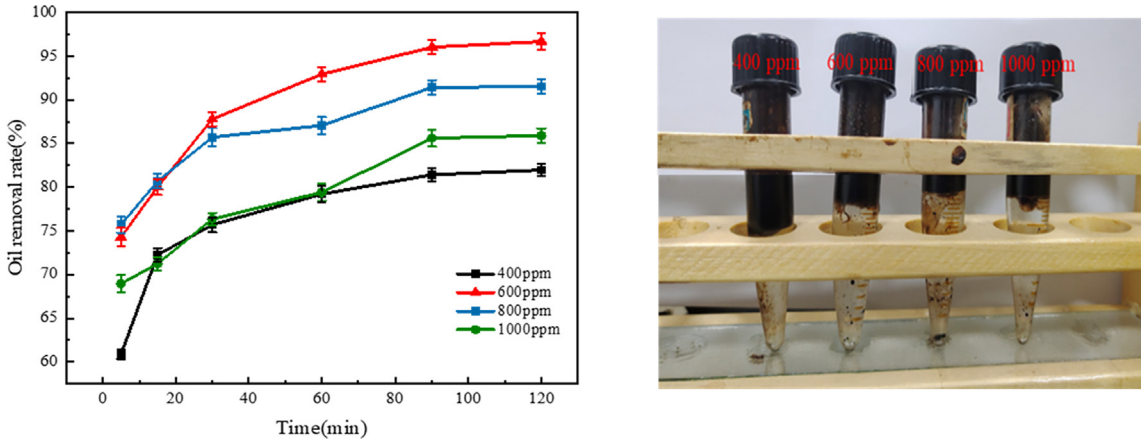

Fig. 5 (a) Demulsification effect of Fe_3O_4@C-F at different dosages, (b) Demulsification effect of different doses of Fe_3O_4@C-F at 120 min.

3.5. Effects of time and temperature on demulsification performance

Four groups of control experiments at different temperatures (35 °C, 50 °C, 65 °C and 80 °C) were set to observe the demulsification effect of Fe_3O_4@C-F within 120 min at 600 ppm demulsifier concentration, the results are shown in Fig. 6. With the increase of demulsification time and temperature, the demulsification efficiency showed an upward trend. When the demulsification temperature was 80 °C and the action time was 120 min, the demulsification efficiency reached the highest. After Fe_3O_4@C-F magnetic demulsifier was added, the emulsion changed rapidly. The color of emulsion changed from dark brown to light brown within 5 min, and the demulsifica-

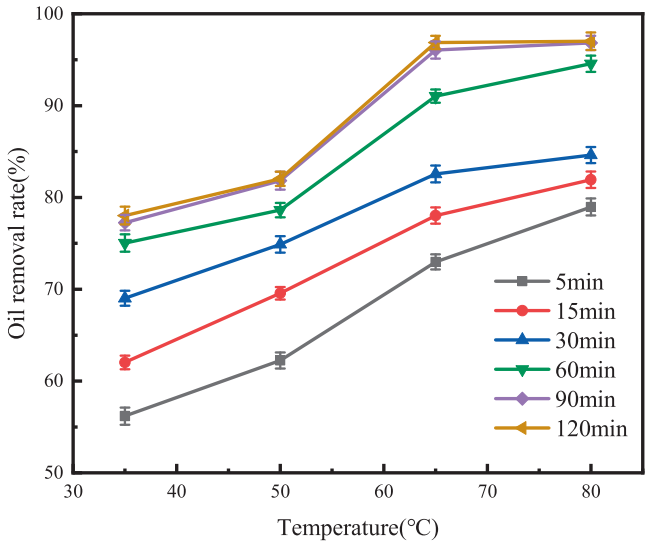

Fig. 6 The demulsification effect of demulsifier with temperature at different time.

tion efficiency exceeded 50%, which reflected the high demulsification efficiency of Fe_3O_4@C-F. Upon reaching a demulsification time of 90 min, the solution exhibited enhanced clarity, accompanied by reduced adhesion of oil droplets. With the increase of action time, the change of solution clarity was not obvious.The horizontal comparison curve showed that although the demulsification efficiency of demulsifier was improved when the action time was extended to 120 min, the increase was not obvious. Similarly, the horizontal comparison curve in Fig. 6 showed that the demulsification efficiency of demulsifier was the best at 80 °C, reaching 97.02%, but it was not significantly improved compared with the demulsification efficiency at 65 °C (96.68%). Obviously, increasing the temperature and prolonging the demulsification time will increase the production cost. Therefore, from the perspective of engineering application, the demulsification time of Fe_3O_4@C-F magnetic demulsifier is set at 90 min and the temperature is set at 65 °C.

3.6. Effect of pH on demulsification performance

Fig. 7(a) shows the effect of Fe_3O_4@C-F magnetic demulsifier on demulsification performance under different pH environments, at the experimental temperature of 65 °C and the dosage of 600 ppm. Fig. 7 (b) shows the demulsification effect of Fe_3O_4@C-F magnetic demulsifier at 65 °C and 600 ppm in different pH environments after 120 min. When the pH value was 6, the demulsification rate of Fe_3O_4@C-F magnetic demulsifier reached the highest and the demulsification performance was the best. Moreover, it demonstrates a remarkable demulsification rate at pH = 5, while exhibiting a demulsification rate exceeding 90% under neutral conditions. These findings signify the exceptional performance of the demulsifier within a neutral to acidic environment. This is because under acidic and neutral conditions, the surface of Fe_3O_4@C-F carries positive charge, while the surface of oil droplets carries negative charge. The electrostatic forces of attraction existing between the two entities facilitate the heightened adsorption of demulsifier molecules onto oil droplets. Furthermore, the presence of dendritic fluorinated polyether on the demulsifier's surface promotes the coalescence of oil droplets, ultimately facilitating efficient oil–water separation. However, the demulsification rate was low when the pH values were 8 and 9, and the demulsification rate was not more than 85%. This is due to the negative charge carried on the surface of Fe_3O_4@C-F under alkaline conditions, and the negative charge carried on the surface of oil droplets occurs electrostatic repulsion, which reduces the adsorption capacity of demulsifiers and leads to the decrease of demulsification rate.

3.7. Recovery performance analysis

The magnetic properties of Fe_3O_4 and its composites were tested by VSM magnetization loop test. The results are shown in Fig. 8(a). Fe_3O_4, Fe_3O_4@C, Fe_3O_4-F and Fe_3O_4@C-F all showed superparamagnetic behavior, and their magnetic saturation values were 65.9, 15.8, 45.8 and 30.6 emu/g, respectively. The composite materials exhibit the superior magnetic saturation value of Fe3O4-F, which can be ascribed to the presence of smaller fluorinated polyether molecules and their

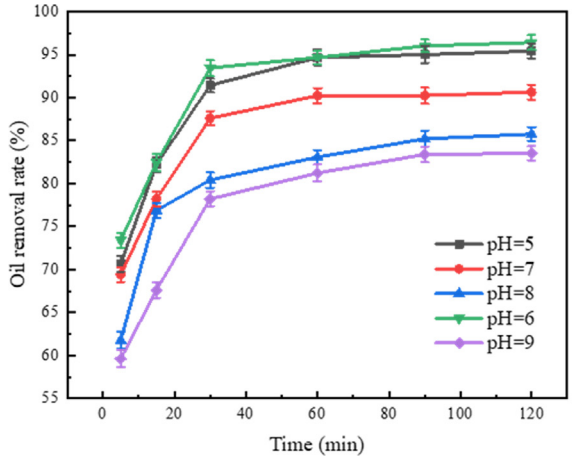

Fig. 7 (a)The demulsification effect of demulsifier at different pH values, (b) Physical diagram of demulsification effect under different pH values in 120 min.

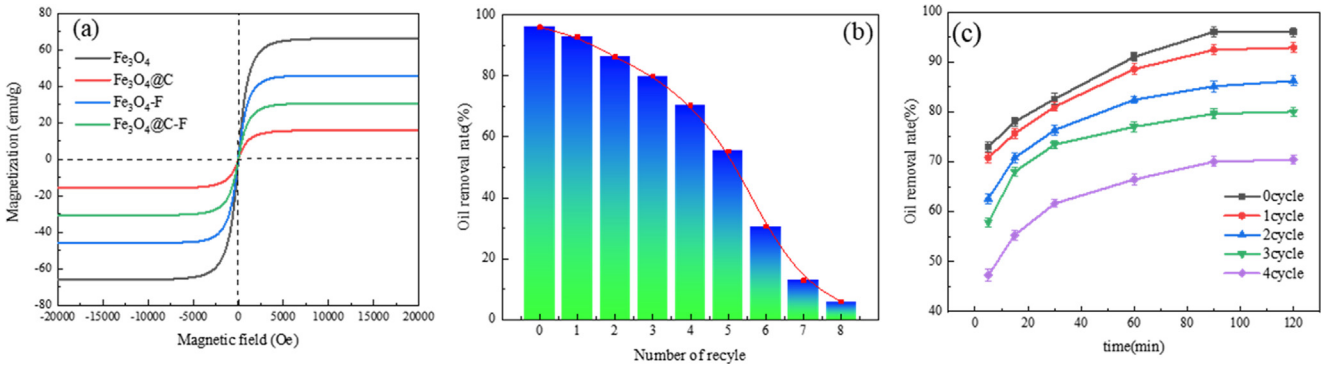

Fig. 8 VSM (a), recovery test (b) and demulsification rate of the first four cycles (c) of Fe_3O_4@C-F.

well-dispersed bonding with the surface of Fe_3O_4 particles. Fe_3O_4@C-F still has magnetic responsiveness, which can be effectively attracted by external magnetic field, and then recycled and reused from the two-phase system. During the recycling examination, the experimental conditions involved a temperature of 65 °C, a demulsifier dosage of 600 ppm, and a reaction time of 90 min. The corresponding outcomes are illustrated in Fig. 8(b). The demulsification efficiency of Fe_3O_4@C-F decreased with the increase of cycles, but it showed excellent demulsification performance in the first four cycles, and the demulsification rates were more than 70%. However, after five times of recycling, the demulsification efficiency of demulsification efficiency dropped sharply, only 12.91% and 5.86% at the 7th and 8th times. The possible reason is that asphalt and resin in crude oil are adsorbed on the surface of demulsifier molecules during demulsification, and n-hexane solvent cannot dissolve all components of crude oil. The decrease of magnetic response leads to the decrease of recovery rate. The demulsification performance of Fe_3O_4@C-F in the first four cycles is shown in Fig. 8(c). Although the demulsification performance of Fe_3O_4@C-F decreased with the increase of the number of cycles, the overall demulsification trend remained unchanged. In summary, Fe_3O_4@C-F magnetic demulsifier not only has excellent demulsification performance, but also has unique magnetic response performance to enable it to be recovered from the oil–water two-phase system by external magnetic field, so as to achieve recyclable recycling. This property solves a series of environmental problems caused by the difficulty of separation of traditional chemical demulsifier after reaction.

3.8. Demulsification mechanism

Fig. 9 shows the demulsification mechanism of Fe_3O_4@C-F magnetic demulsifier. Firstly, due to the existence of C-F bond, Fe_3O_4@C-F magnetic demulsifier has ultra-high surface activity. When Fe_3O_4@C-F enters the crude oil emulsion, it can quickly reach the oil–water interface film, and then replace the natural emulsifiers such as asphaltenes and colloids on the oil–water interface film to form a fragile film. The branched fluorinated polyether on the surface of magnetic demulsifier can act as a bridge to promote the oil droplet coalescence. Secondly, carbon oxide nanospheres have a conjugated aromatic ring structure, which can adsorb oil droplets

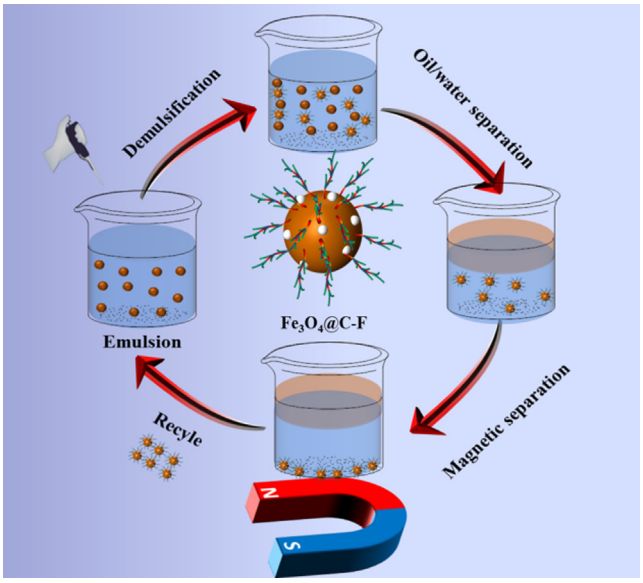

Fig. 9 Demulsification mechanism of Fe_3O_4@C-F.

in the emulsion through a strong π-π interaction with organic compounds such as asphaltene and colloid. Then, Fe_3O_4 has the characteristics of superhydrophobicity. It carries positive charges under acidic and neutral conditions, and can attract oil droplets carrying negative charges through electrostatic interactions, which improves the adsorption capacity of Fe_3O_4@C-F. Moreover, the nanoscale characteristics of carbon nanospheres and Fe_3O_4 provide a considerable adsorption area. This unique combination enables a synergistic demulsification effect. It can be seen from TEM and particle size distribution that the particle size of Fe_3O_4@C-F is relatively uniform. The introduction of Fe_3O_4 and carbon nanospheres provides more sites for the grafting of fluorinated polyether. Finally, Fe_3O_4@C-F has magnetic response, which can be recovered from the two-phase system under the action of external magnetic field and recycled after cleaning.

4. Conclusion

This study used a straightforward solvothermal method to create a new kind of effective and environmentally friendly demulsifier based on the original fluorinated polyether demulsifier and the inventive

addition of Fe_3O_4 and carbon elements. The demulsification effect of Fe_3O_4@C-F in 120 min can reach 96.68% when the demulsifier dosage is 600 ppm, the test temperature is 65 °C, and the pH = 6. In addition, Fe_3O_4@C-F can be recycled from the two-phase system for 5 times under an external magnetic field. The excellent demulsification performance of Fe_3O_4@C-F is attributed to the high surface activity. Carbon nanospheres and Fe_3O_4 are nano-sized particles with large specific surface area and many adsorption sites, which play a synergistic role. We also found that the demulsifier can quickly reach the oil–water interfacial film after adding into the crude oil emulsion, and replace the natural emulsifiers such as asphaltenes and colloids on the oil–water interfacial film to form a new easily fractured film. In addition, we also carried out the magnetic response recovery experiment. The application of carbon nanomaterials in demulsification not only broadens the application scope of carbon nanomaterials, but also provides a new idea for the application of efficient demulsifiers.

CRediT authorship contribution statement

Xinlei Jia: Conceptualization, Methodology. **Lixin Wei:** Software, Supervision. **Mingming Fu:** Validation, Formal analysis. **Chao Liu:** Software, Data curation. **Yuxin Gu:** Investigation. **Weining Qin:** Investigation. **Lin Zhang:** Investigation, Software. **Xiaoheng Geng:** Investigation, Software. **Haiying Guo:** Investigation, Software.

Declaration of Competing Interest

The authors declare that they have no known competing financial interests or personal relationships that could have appeared to influence the work reported in this paper.

Acknowledgments

The authors are grateful for the reviewers' instructive suggestions and careful proofreading. This work was supported by the Natural Science Foundation of Shandong Province for Youth (Grant No. ZR2020QE111), The key experimental technology project of Binzhou University 'Reform and Exploration of Experimental Teaching Mode of Safety Engineering Specialty under the Background of New Engineering' (Grant No. BZXYSYXM202104), the National Natural Science Foundation of China Youth Fund (52004031) and the Postdoctoral Science Foundation of China (2020M681073).

Appendix A. Supplementary material

Supplementary data to this article can be found online at https://doi.org/10.1016/j.arabjc.2023.105134.

References

Alves, A.V., Tsianou, M., Alexandridis, P., 2020. Fluorinated surfactant adsorption on mineral surfaces: implications for pfas fate and transport in the environment. Surfaces 3 (4), 516–566. https://doi.org/10.3390/surfaces3040037.

Bélarbi, H., Bendedouch, D., Bouanani, F., 2010. Mixed micellization properties of nonionic fluorocarbon/cationic hydrocarbon surfactants. J. Surfactants Deterg. 13 (4), 433–439. https://doi.org/10.1007/s11743-010-1191-x.

Fang, S., Chen, B., Chen, T., Duan, M., Xiong, Y., Shi, P., 2017. An innovative method to introduce magnetism into demulsifier. Chem. Eng. J. 314, 631–639. https://doi.org/10.1016/j.cej.2016.12.023.

Feng, X.J., He, X., Lai, L., Lu, Q., Wu, J., 2021. Polydopamine-anchored polyether on fe3o4 as magnetic recyclable nanoparticle-demulsifiers. Colloids Surf., A. 617, 126142. https://doi.org/10.1016/j.colsurfa.2021.126142.

Gasanov, A.A., Dashdiyeva, T.K., Dashdiyev, R.A., 2019. Evaluation of novel nanodemulsifier based on colloidal and non-colloidal surfactants for the removal of hydrocarbons from wastewater. J. Water. Chem. Technol. 41 (6), 377–383. https://doi.org/10.3103/S1063455X19060067.

Geng, X., Li, C., Zhang, L., Guo, H., Shan, C., Jia, X., Cai, Y., Han, L., 2022. Screening and demulsification mechanism of fluorinated demulsifier based on molecular dynamics simulation. Molecules 27 (6), 1799. https://doi.org/10.3390/molecules27061799.

Guo, Y., Surblys, D., Matsubara, H., Ohara, T., 2021. A molecular dynamics study of the effect of functional groups and side chain on adsorption of alcoholic surfactant and interfacial thermal transport. J. Mol. Liq. 335 (1), 116243. https://doi.org/10.1016/j.molliq.2021.116243.

He, D., Li, L., Bai, F., Zha, C., Bao, N., 2016. One-pot synthesis of pomegranate-structured Fe_3O_4/carbon nanospheres-doped graphene aerogel for high-rate lithium ion batteries. Chemistry 22 (13), 4454–4459. https://doi.org/10.1002/chem.201504429.

Hjartnes, T.N., Srland, G.H., Simon, S.C., Sjoblom, J., 2019. Demulsification of crude oil emulsions tracked by pulsed field gradient NMR. Part I: chemical demulsification. Ind. Eng. Chem. Res. 58 (6), 2310–2323. https://doi.org/10.1021/acs.iecr.8b05165.

Hu, M., Jing, L., An, Q., Ming, W., Bian, C., Chen, M., 2017. Tribological properties and milling performance of hss-co-e tools with fluorinated surfactants-based coatings against ti–6al–4v. Wear. 376, 134–142. https://doi.org/10.1016/j.wear.2017.01.025.

Huan, W., Zhang, J., Qin, H., Fei, H., Wang, B., Wu, M., Li, J., 2019. A magnetic nanofiber-based zwitterionic hydrophilic material for the selective capture and identification of glycopeptides. Nanoscale 11 (22), 10952–10960. https://doi.org/10.1039/C9NR01441A.

Huang, B., Li, X., Zhang, W., Fu, C., Wang, Y., Fu, S., 2019. Study on demulsification-flocculation mechanism of oil-water emulsion in produced water from alkali/surfactant/polymer flooding. Polymers 11 (3), 395. https://doi.org/10.3390/polym11030395.

Huang, Z., Li, P., Luo, X., Jiang, X., Liu, L., Ye, F., 2019. Synthesis of a novel environmentally friendly and interfacially active cnts/sio_2 demulsifier for w/o crude oil emulsion separation. Energy Fuels. 33 (AUG.), 7166–7175. https://doi.org/10.1021/acs.energyfuels.9b01217.

Khan, J.A., Al-Kayiem, H.H., Aleem, W., Saad, A.B., 2019. Influence of alkali-surfactant-polymer flooding on the coalescence and sedimentation of oil/water emulsion in gravity separation. J. Pet. Sci. Eng. 173, 640–649. https://doi.org/10.1016/j.petrol.2018.10.055.

Li, S., Li, N., Yang, S., Liu, F., Zhou, J., 2013. The synthesis of a novel magnetic demulsifier and its application for the demulsification of oil-charged industrial wastewaters. J. Mater. Chem. A. 2 (1), 94–99. https://doi.org/10.1039/C3TA12952G.

Mu, Y., Liu, J., Liu, J., Ren, S., 2022. Preparation and demulsification performance of modified attapulgite nanoparticle demulsifier. Fuel 313, 123038. https://doi.org/10.1016/j.fuel.2021.123038.

Nab, A., Aaa, B., 2022. Synthesis of novel demulsifier nano-materials and their application in the oil industry. Mater. Today: Proc. 49, 2842–2850. https://doi.org/10.1016/j.matpr.2021.10.069.

Nikkhah, M., Tohidian, T., Rahimpour, M.R., Jahanmiri, A., 2015. Efficient demulsification of water-in-oil emulsion by a novel nano-titania modified chemical demulsifier. Chem. Eng. Res. Des. 94, 164–172. https://doi.org/10.1016/j.cherd.2014.07.021.

Peyre, V., 2009. Segregation phenomena in micelles from mixtures of fluorinated and hydrogenated surfactants. Curr. Opin. Colloid Interface Sci. 14 (5), 305–314. https://doi.org/10.1016/j.cocis.2009.05.010.

Shuying, H.e., Kun, G., 2021. What factors contribute to the mutual dependence degree of China in its crude oil trading relationship

with oil-exporting countries?. Energy 228, 120547. https://doi.org/10.1016/j.energy.2021.120547.

Suhaimin, N.S., Jaafar, J., Aziz, M., Ismail, A.F., Yusof, N., 2021. Nanocomposite membrane by incorporating graphene oxide in sulfonated polyether ether ketone for direct methanol fuel cell. Mater. Today: Proc. 46, 2084–2091. https://doi.org/10.1016/j.matpr.2021.03.614.

Umar, A.A., Saaid, I.M., Halilu, A., Sulaimon, A.A., Ahmed, A.A., 2020. Magnetic polyester bis-mpa dendron nanohybrid demulsifier can effectively break water-in-crude oil emulsions. sciencedirect. J. Mater. Res. Technol. 9 (6), 13411–13424. https://doi.org/10.1016/j.jmrt.2020.09.074.

Velayati, A., Nouri, A., 2021. Role of asphaltene in stability of water-in-oil model emulsions: the effects of oil composition and size of the aggregates and droplets. Energy Fuels 35 (7), 5941–5954. https://doi.org/10.1021/acs.energyfuels.1c00183.

Wang, Z.M., Zhang, J., 2016. Corrosion of multiphase flow pipelines: the impact of crude oil. Corrosion Rev. 34 (1–2), 17–40. https://doi.org/10.1515/corrrev-2015-0053.

Wei, L., Zhang, L., Chao, M., Jia, X., Shi, L., 2021. Synthesis and study of a new type of nonanionic demulsifier for chemical flooding emulsion demulsification. ACS Omega 6 (27), 17709–17719. https://doi.org/10.1021/acsomega.1c02352.

Xie, Y., Deng, C., 2017. Designed synthesis of a "one for two" hydrophilic magnetic amino-functionalized metal-organic framework for highly efficient enrichment of glycopeptides and phosphopeptides. Sci. Rep. 7 (1), 1162. https://doi.org/10.1038/s41598-017-01341-y.

Xu, Z., Wu, Y., Deng, Z., Long, J., Deng, C., 2021. One-step fabrication of strongly hydrophilic mesoporous silica for comprehensive analysis of serum glycopeptidome. Talanta 234, 122713. https://doi.org/10.1016/j.talanta.2021.122713.

Yin, 2014. Synthesis and demulsification performance of multi-branch block polyether. (Doctoral dissertation, Shandong University).

Zhang, J., Wang, Y., Xu, G., Lin, M., Fan, T., Yang, Z., 2016. Formation and rheological behavior of wormlike micelles in a catanionic system of fluoroacetic acid and tetradecyldimethylaminoxide. Soft Matter. 13 (3), 670–676. https://doi.org/10.1039/C6SM02653B.

Zhang, J., Ge, D., Wang, X., Wang, W., Zhang, W., 2021. Influence of surfactant and weak-alkali concentrations on the stability of o/w emulsion in an alkali-surfactant–polymer compound system. ACS Omega. 6 (7), 5001–5008. https://doi.org/10.1021/acsomega.0c06142.

Zhang, L., Ying, H., Yan, S., Zhan, N., Guo, Y., Fang, W., 2018. Hyperbranched poly (amido amine) demulsifiers with ethylenediamine/1,3-propanediamine as an initiator for oil-in-water emulsions with microdroplets. Fuel. 226, 381–388. https://doi.org/10.1016/j.fuel.2018.03.196.

Zhao, N., Wu, S., He, C., Wang, Z., Shi, C., Liu, E., 2013. One-pot synthesis of uniform Fe_3O_4 nanocrystals encapsulated in interconnected carbon nanospheres for superior lithium storage capability. Carbon 57, 130–138. https://doi.org/10.1016/j.carbon.2013.01.056.

Zhao, B., Zhang, X., Fu, X., Mccarthy, C., 2019. Synthesis of fe_3o_4 hollow nanospheres-carbon nanotubes nanocomposites for the enhancement of dielectric heating performance. Mater. Lett. 235, 31–34. https://doi.org/10.1016/j.matlet.2018.09.155.

Zhou, J., Sui, H., Ma, J., Li, X., He, L., 2021. Fast demulsification of oil-water emulsions at room temperature by functionalized magnetic nanoparticles. Sep. Purif. Technol. 274, 118967. https://doi.org/10.1016/j.seppur.2021.118967.